(0) 4 pages

Characterization of the structural and electrical properties of ion beam sputtered ZnO films

Peter P. Murmu[1,2,3,a], John Kennedy[1,2,b], Ben J. Ruck[2,3] and Andreas Markwitz[1,2]

[1]National Isotope Centre, GNS Science, PO Box 31312, Lower Hutt, New Zealand

[2]The MacDiarmid Institute for Advanced Materials and Nanotechnology, New Zealand

[3]School of Chemical and Physical Sciences, Victoria University of Wellington, PO Box 600, Wellington, New Zealand

[a]p.murmu@gns.cri.nz, [b]j.kennedy@gns.cri.nz

Keywords: ZnO, Ion Beam Sputtering, XRD, AFM, Resistivity, Carrier concentration

Abstract. We report the structural and electrical properties of ion beam sputtered ZnO films vacuum annealed at varying temperatures. XRD results revealed that the films grow along the *c*-axis. The crystallite sizes increase from ~8 to ~30 nm upon annealing at 800 °C. Annealing aided to recover the compressive strain and regain the standard lattice parameter values. The RMS surface roughness increased to ~5.0 nm after annealing at 800 °C as observed in AFM micrographs. Increased resistivity on the annealed films suggested that the oxygen vacancies are compensated by de-trapped oxygen at grain boundaries.

Introduction

Zinc oxide (ZnO) is a promising II-VI group oxide semiconductor owing to its direct band gap and large free-exciton binding energy [1], with various potential applications such as in liquid crystal displays [1], light emitting diodes [2], piezoelectric transducers [3], UV/gas sensors [4], solar cells [5] etc. Its high radiation resistance property can be utilized in applications at elevated temperatures [6]. It possesses a wurtzite crystal structure with lattice parameters a=3.2498 Å and c= 5.2066 Å. ZnO film preparation techniques include the sol-gel process [7], chemical vapour deposition (CVD) [8], pulsed laser deposition (PLD) [9], molecular beam epitaxy (MBE) [10], and sputtering [11].

ZnO usually shows *n*-type conductivity due to the presence of intrinsic defects such as oxygen vacancies and zinc interstitials [1, 12]. It is reported to play a crucial role in dilute magnetic semiconductors (DMSs) in which the spin of electron would be utilized in addition to the charge [1]. The magnetic impurities are introduced by doping transition metal or rare-earth elements in the conventional semiconductors. The defects in ZnO can significantly influence the electrical and magnetic properties [1, 12]. Therefore, it is important to investigate the evolution of the defects in undoped films with respect to annealing temperatures. In this paper we report the structural and electrical properties upon vacuum annealing on the ZnO films prepared by ion beam sputtering (IBS).

Experiment

ZnO thin films were deposited by ion beam sputtering onto silicon (Si) and silicon dioxide on Si (SiO_2/Si) substrates at ambient temperature. The sputtering was carried out using a 10 keV Ar^+ beam at high vacuum (base pressure ~10^{-7} mbar). Detailed reports of film deposition by the ion beam sputtering technique are presented elsewhere [13]. Films were subsequently subjected to high vacuum annealing for 30 minutes at various temperatures. Rutherford backscattering spectrometry (RBS) measurements were carried out for compositional and depth profile analyses with a 2 MeV He^+ beam using the 3 MeV Van de Graff accelerator at GNS Science, Lower Hutt, New Zealand [14]. Thickness of the films was found ~150 nm. Surface morphology was characterized by atomic force microscopy (Nanosurf EasyScan 2) in contact mode over a range of 5x5 μm^2. Crystal structures were studied using X-ray diffraction (XRD) utilizing Cu K_α radiation. Hall-effect and

resistivity measurements were conducted using the four probe van der Pauw method at ambient temperature.

Results and Discussion

The crystalline structure and orientation of the as-deposited and annealed ZnO films were investigated using X-ray diffraction, as shown in Figure 1. All films are polycrystalline with major peaks attributable to (100), (002), and (101) planes of hexagonal ZnO, as determined using the Joint Committee of Powder Diffraction Standards (JCPDS) file [15]. In each case the strongest peak corresponds to (002) suggesting strong *c*-axis orientation. Usually, films grow along a particular direction in order to minimize the surface free energy. Fujimura et al. [16] showed that the (002) plane has the lowest surface free energy, 0.009 eV/Å^2, compared to the (110) and (100) planes which have surface free energies of 0.123 and 0.209 eV/Å^2 respectively, consistent with the observations.

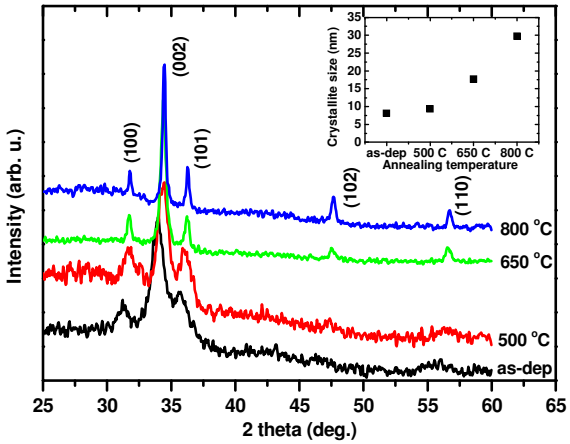

Fig. 1. XRD spectra of as-deposited and annealed ZnO films.

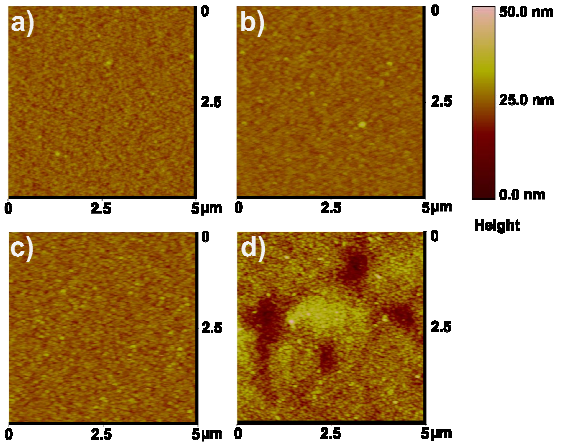

Fig. 2. AFM images of (a) as-deposited, (b) 500 °C, (c) 650 °C, and (d) 800 °C annealed ZnO films.

The lattice parameters *a* and *c* can be calculated using $a=\lambda/(1.732\sin\theta)$ and $c=\lambda/(\sin\theta)$ respectively, where λ is the X-ray wavelength and θ the Bragg angle [17]. For an as-deposited film they are found to be *a*=3.297 Å and *c*= 5.273 Å, somewhat larger than the lattice parameters for pure ZnO (*a*=3.2498 Å and *c*= 5.2066 Å) [1]. We attribute the almost uniform lattice expansion to a high density of point defects in the as-grown films. Annealing at 800 °C reduced these values to *a*=3.25 Å and *c*= 5.204 Å, much closer to the bulk values, consistent with the recovery of point defects. The average crystallite size can be calculated using Scherrer's formula, $d=0.9\lambda/(\beta\cos\theta)$, where λ is the X-ray wavelength, β the FWHM of 2θ in radians and θ the Bragg angle [17]. The crystallite sizes of as-deposited and annealed films are shown in the inset of the figure 1. For an as-deposited film it is found ~8.0 nm which increases to ~30 nm upon annealing the film at 800 °C.

AFM measurements were performed to study the microstructural evolution of the surface morphology in as-deposited and annealed films, as shown in Figure 2. The root mean square (RMS) roughness for an as-deposited film was found ~1.7 nm. Annealing temperatures up to 650 °C, had no significant impact on the RMS roughness. However, at 800 °C the RMS roughness increased up to 5.0 nm. It is observed that annealing leads to the formation of larger grains which grow along the *c*-axis or perpendicular to the sample surface. An increment in the size of grains/crystallites along the *c*-axis can lead to a substantially rough surface.

Hall-effect measurements were conducted to investigate the electrical properties of the films. The measurements were carried out at ambient temperature with an applied field of 0.55 Tesla. All the films exhibited *n*-type conductivity which is usually attributed to the intrinsic defects present in the ZnO films [1, 12]. Figure 3 shows the resistivity and carrier concentration obtained for the as-deposited and annealed films. The as-deposited film is found to be the most conductive with the highest carrier concentration. The resistivity and carrier concentration values were found ~1.7 x 10^{-2} Ωcm and ~ 1.27 x 10^{20} cm^{-3} respectively. The annealing increased the resistivity by up to 3 orders of magnitude and reduced the carrier concentration by more than 2 orders of magnitude. Oxygen vacancies are reported to trap electrons and create deep levels in the band gap [18]. Annealing in vacuum increases the number of oxygen vacancies due to diffusion towards the surface leading to increased charge carriers and lower resistivity. However, the opposite trend is observed in the annealed films, as the resistivity increased upon annealing. Kim et al. [19] observed a similar trend of increasing resistivity with annealing temperature in polycrystalline ZnO films prepared by plasma-enhanced chemical vapour deposition (PECVD). They suggested that the oxygen vacancies can be annihilated by de-trapped oxygen atoms at grain boundaries during annealing. XRD measurements indeed showed the growth of grain sizes upon annealing and possibly release of oxygen atoms at grain boundaries helped to compensate the oxygen vacancies.

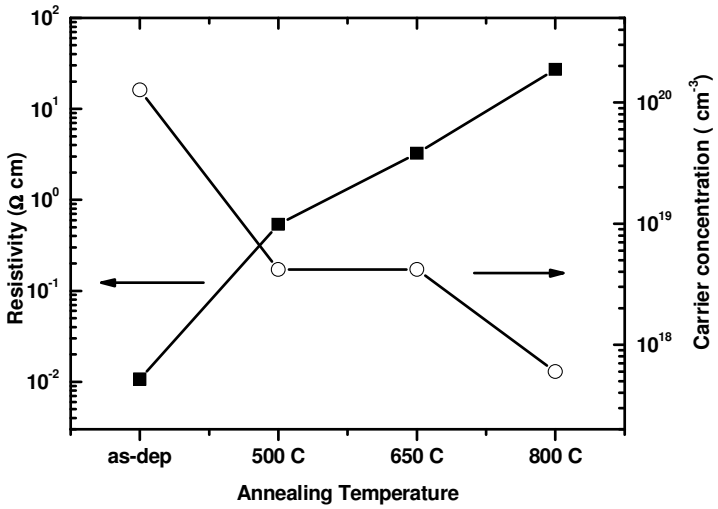

Fig. 3. Resistivity and carrier concentration of as-deposited and annealed ZnO films. Lines are guide to the eyes.

Summary

In summary, the structural and electrical properties of the ion beam sputtered ZnO films are reported. XRD spectra revealed the improvement of crystalline quality upon annealing and growth of larger crystallites along the *c*-axis. A reduction in lattice parameter was observed due to reduced compressive strain. AFM micrographs showed the RMS surface roughness increased to 5.0 nm upon annealing at 800 °C. Increased resistivity due to annealing can be associated with the annihilation of oxygen vacancies due to de-trapped oxygen at the grain boundaries.

Acknowledgement

This work is carried out with a research contract from Foundation for Research Science and Technology of New Zealand (C05X0408) and the MacDiarmid Institute for PhD scholarship.

References

[1] U. Ozgur, Y.I. Alivov, C. Liu, A. Teke, M.A. Reshchikov, S. Dogan, V. Avrutin, S.J. Cho, H. Morkoc, J. Appl. Phys. 98 (2005) 041301.

[2] T. Pauporte, D. Lincot, B. Viana, F. Pelle, Appl. Phys. Lett. 89 (2006) 233112.

[3] J.J. Chen, F. Zeng, D.M. Li, J.B. Niu, F. Pan, Thin Solid Films 485 (2005) 257–261.

[4] F. Fang, J. Futter, A. Markwitz, J. Kennedy, Nanotechnology 20 (2009) 245502.

[5] T. Yoshida, J. Zhang, D. Komatsu, S. Sawatani, H. Minoura, T. Pauporte, D. Lincot, T. Oekermann, D. Schlettwein, H. Tada, D. Wohrle, K. Funabiki, M. Matsui, H. Miura, H. Yanagi, Adv. Funct. Mater. 19 (2009) 17–43.

[6] S.O. Kucheyev, J.S. Williams, C. Jagadish, J. Zou, C. Evans, A.J. Nelson, A.V. Hamza, Phys. Rev. B 67 (2003) 094115.

[7] Z.B. Shao, C.Y. Wang, S.D. Geng, X.D. Sun, S.J. Geng, J. Mater. Process. Technol. 178 (2006) 247.

[8] J.G. Lu, T. Kawaharamura, H. Nishinaka, Y. Kamada, T. Ohshima, S. Fujita, J. Cryst. Growth 299 (2007) 1.

[9] R. Perez-Casero, A. Gutierrez-Llorente, O. Pons-y-Moll, W. Seiler, R.M. Defourneau, D. Defourneau, E. Millon, J. Perriere, P. Goldner, B. Viana, J. Appl. Phys. 97 (2005) 054905.

[10] D.C. Oh, T. Suzuki, J.J. Kim, H. Makino, T. Hanada, M.W. Cho, T. Yao, Appl. Phys. Lett. 86 (2005) 032909.

[11] E.M. Bachari, G. Baud, S. Ben Amor, M. Jacquet, Thin Solid Films 348 (1999) 165-172.

[12] D.C. Look, J.W. Hemsky, J.R. Sizelove, Phys. Rev. Lett. 82 (1999)2552–2555

[13] J. Kennedy, J. Pithie, A. Markwitz, Proc. of SPIE Vol. 6800 (2008) 68001P-1-8.

[14] J. Kennedy, A. Markwitz, H.J. Trodahl, B.J. Ruck, S.M. Durbin, W. Gao, J. Electronic Materials 36(4) (2007) 472-482.

[15] JCPDS, Joint Committee for Powder Diffraction Standards, Powder Diffraction File for Inorganic Materials, 79-2205 (1979).

[16] N. Fujimura, T. Nishihara, S. Goto, J. Xu, T. lto, J. Crys. Growth 130 (1993) 269-279.

[17] B.D. Cullity, Elements of X-Ray Diffractions, Addison-Wesley, Reading, MA, 1978.

[18] K. Vanheusden, W.L. Warren, C.H. Seager, D.R. Tallant, J.A. Voigt, B.E. Gnade, J. Appl. Phys. 79 (10) 7983.

[19] Y.J. Kim, H.J. Kim, Materials Letters 41 (1999) 159–163.